Terahertz Emission from Quantum Cascade Lasers in the Quantum Hall Regime: Evidence for Many Body Resonances and Localization Effects

Giacomo Scalari,* Stéphane Blaser,† and Jérôme Faist‡

Institute of Physics, University of Neuchâtel, CH-2000 Neuchâtel, Switzerland

Harvey Beere, Edmund Linfield, and David Ritchie

Cavendish Laboratory, University of Cambridge, Madingley Road, Cambridge CB3 0HE, United Kingdom

Giles Davies

School of Electronic and Electrical Engineering, University of Leeds, Leeds LS2 9JT, United Kingdom

(Received 17 March 2004; revised manuscript received 14 July 2004; published 1 December 2004)

A terahertz quantum cascade laser, operating at $\lambda = 159\ \mu$m and exploiting the in-plane confinement arising from perpendicular magnetic field, is used to investigate the physics of electrons confined on excited subbands in the regime of a large ratio of the magnetic field confinement energy to the photon energy. As the magnetic field is increased above about 6 T, and the temperature lowered below 20 K, the devices are characterized by a very low threshold current density, with values as low as $J_{\mathrm{th}} = 1\mathrm{A/cm}^2$, and an increase of gain by five times the low field value. We show that, as with the quantum Hall effect, the key physical process is the localization of the carriers. Evidences for resonant electron-electron scattering processes are directly obtained from light intensity and transport measurements.

DOI: 10.1103/PhysRevLett.93.237403 PACS numbers: 78.60.Fi, 42.55.Px, 85.30.Tv, 95.85.Gn

The quantum cascade (QC) laser [1] is a coherent source of infrared radiation based on quantum confinement and tunneling in semiconductor heterostructures. Gain arises from a population inversion between two-dimensional subbands. This continuum of available states provided by the free in-plane motion of the carriers is responsible for two strong limitations of quantum cascade lasers structures: the relatively short upper state lifetime and the waveguide losses arising from free carrier absorption.

Strong in-plane quantization, through which the in-plane parabolic dispersion becomes a set of discrete levels, is potentially able to change this picture by acting on the fundamental process governing the lifetime τ of the intersubband transition. The application of a strong perpendicular magnetic field provides a tunable confinement, by breaking the free-electron in-plane dispersion, with energy $E_{i,k} = E_i + (\hbar^2 k^2)/2m^*$, of each of the two-dimensional states into a set of equidistant Landau levels [$|i, n\rangle$ with $E_{i,n} = E_i + (n + \frac{1}{2})\hbar\omega_c$] separated by the cyclotron energy $\hbar\omega_c = (\hbar eB)/m^*$.

In previous experiments, modifications of the characteristics of a QC laser (both mid-IR and THz) have been studied for cyclotron energies smaller or equal to the photon energy [2–5]. In a recent work, the modification of scattering times by Landau levels has been exploited to enhance the population inversion in a QC laser [6] based on an intersubband transition between the first two excited states of a thick quantum well. We investigate in this Letter such a device, designed to operate at 1.9 THz (7.9 meV, $\lambda \simeq 160\ \mu$m) in the regime of strong magnetic confinement. The temperatures, mobilities, and magnetic fields correspond to the physics of resonant tunneling in the quantum Hall regime [7]. In contrast to previous work, where an intermediate regime was achieved in which the magnetic confinement was strong enough to modulate the intersubband lifetime but no qualitative change was observed in the laser behavior, we are able to demonstrate two dramatic new features unique to devices operating in this strong field regime: a strong reduction of the waveguide losses and an increase in the gain attributed to carrier localization, and a resonant electron-electron scattering effect.

As shown schematically in the inset of Fig. 1(a), the active region of our device, similar in concept to the one presented in Ref. [6], consists of a 55 nm thick undoped GaAs quantum well followed in sequence by a coupled well extractor and a three quantum well injector. The exact layer sequence is given in the caption of Fig. 1. As shown in Fig. 1(d), where a Landau fan of the active region is plotted, the device is originally designed to operate at a field of 2.9 T where the cyclotron energy matches the E_{21} energy spacing, reducing the $n = 2$ lifetime. At the same time, the energy spacings E_{32} and E_{31} are, respectively, equal to one and a half times and two and a half times the cyclotron energy, enhancing the $n = 3$ lifetime. This combination of level alignment therefore enhances the $n = 3$ to $n = 2$ population inversion.

The structure was grown by molecular beam epitaxy on a semi-insulating GaAs substrate. One hundred periods of the active region were deposited between 0.7 μm thick (Si doped, 9×10^{17} cm^{-3}) lower and 0.08 μm thick (Si doped, 5×10^{18} cm^{-3}) upper GaAs contact layers. The devices were then processed into 100–520 μm wide and 0.5–4.7 mm long ridge stripes by wet chemical etching. After thinning to a substrate thickness of

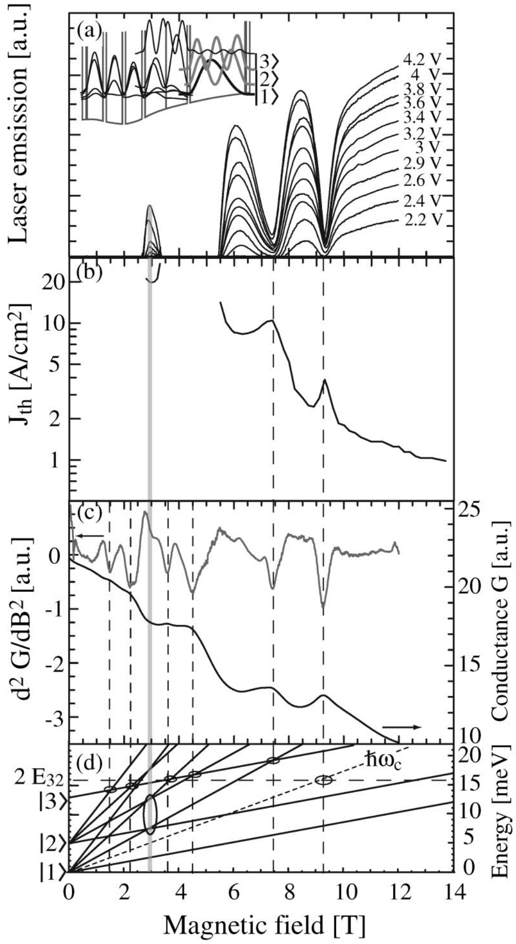

FIG. 1. (a) Light emission in pulsed mode as a function of magnetic field for various applied biases for a 3.5 mm long, 520 μm wide laser stripe with backfacet high reflection (HR) coating at 4.2 K. Inset: band structure of one period of the active region; the layer sequence in nm starting from the injection barrier is (from right to left) as follows: **2.5**/3.5/**1.2**/55.0/**3**/21.0/**1.0**/20.0/**3.2**/16.4/**3.2**/16.0/**3.5**/15.8/**1.0**/3.8/ (underlined layers are Si doped at 1.5×10^{16} cm^{-3}; figures in bold type are $Al_{0.15}Ga_{0.85}As$ layers). (b) Threshold current density as a function of magnetic field for the same device as in (a). (c) Conductance (black line), together with its second derivative (grey line), as a function of magnetic field at 4.2 K measured on a 320×400 μm^2 mesa at 1.5 V applied bias. (d) Landau fan plot of the active region: the dashed line is the cyclotron energy. Note the crossing at 9.3 T of the cyclotron energy with the horizontal wide dashed line representing two times the photon energy $2E_{32}$.

100 μm and back metallization, the devices were indium soldered onto copper heatsinks and inserted into the bore of a superconducting cryostat [6]. The optical waveguide exploited the second order mode of the metal-semiconductor-metal waveguide formed by the top and substrate metallizations, as shown in the inset of Fig. 2(a). Light intensity characteristics, obtained by ramping the magnetic field applied perpendicularly to the epilayers, are displayed in Fig. 1(a) for various applied biases. As expected, the device displays a first maximum of intensity at an applied magnetic field of 2.9 T, corresponding to the design field at which the lifetime of the $n = 2$ state is reduced by enhanced scattering [8] at the crossing of the Landau levels $|1, i\rangle \rightarrow |2, i-1\rangle$. The laser then switches off until a field value of 5.5 T, at which point a series of oscillations starts. As shown in Fig. 1, the extinction of the laser between 3.3 and 5.5 T, as well as the minimum at 7.4 T, can be attributed to resonances between the $n = 3$ state and an excited Landau level of the $n = 1$ and $n = 2$ levels, and $n = 1$ level, respectively [3–6,9]. For fields larger than 3 T, $\hbar\omega_c > E_{21}$ and no resonances between the $n = 2$ and $n = 1$ states are allowed.

The conductance, measured directly by a lock-in technique, is displayed in Fig. 1(c), together with its second derivative in magnetic field $\frac{\partial^2 G}{\partial B^2}$. This quantity reflects the variation of the $n = 3$ lifetime with applied magnetic field. As expected, an excellent agreement is found between the conductance and laser emission data whenever a Landau level crossing involving the $n = 3$ state occurs.

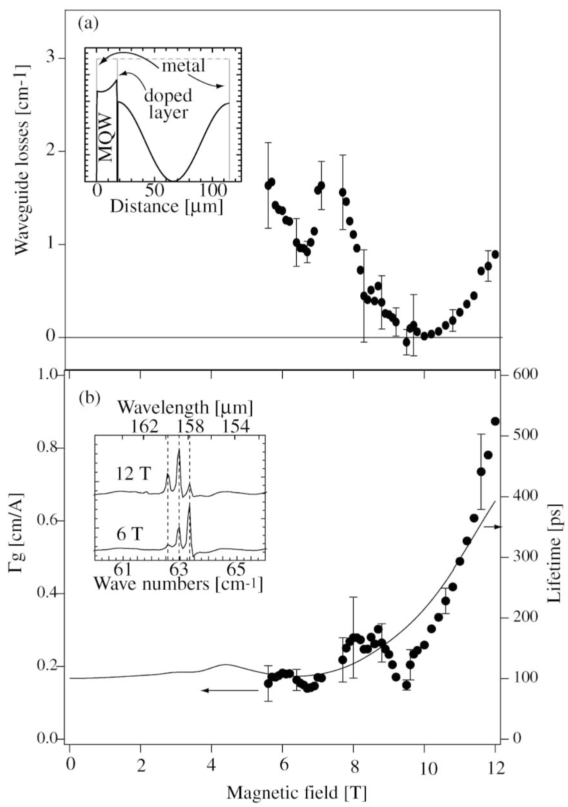

FIG. 2. (a) Waveguide losses as a function of magnetic field for a ridge width of 420 μm. Inset: intensity profile for the $n = 2$ TM mode (black line) which has a calculated value of losses of 7.9 cm^{-1} and a mode overlap of $\Gamma = 0.29$. (b) Left axis (disks): modal gain as a function of applied magnetic field for a ridge width of 420 μm. Right axis (full line): lifetime deduced from the magnetotransport of the diagonal terahertz emitter studied in Ref. [16]. Inset: laser spectra recorded at six and 12 T for a 3.4 mm long, 220 μm wide cavity at $T = 4.2$ K with an FTIR spectrometer (resolution 0.125 cm^{-1}).

The minimum at 7.4 T marks the crossing of the first excited Landau level of state one with the ground Landau level of state three $|3, 0\rangle \longrightarrow |1, 1\rangle$ above which the in-plane confinement energy is greater than E_{31}. For this reason, for fields larger than 7.4 T, no more inter-Landau-level resonances should be observed. However, a very strong feature is present at 9.3 T, corresponding to a field where the photon energy is half of the cyclotron energy, $\hbar\omega_c(9.3\ \mathrm{T}) = 15.9\ \mathrm{meV} = 2h\nu = 2E_{32}$. In fact, this resonance was predicted theoretically [10] as a signature of an electron-electron scattering event in which energy and momentum are conserved with one electron scattering to the lower Landau level and a second electron scattering up to the higher Landau level. A signature of this effect in transport only was observed previously at very large magnetic field values [10]. In our data, this resonance appears not only in transport but also in the light intensity for the first time.

The threshold current density J_{th} of the device [Fig. 1(b)] also exhibits the resonances displayed in the light intensity data, and steadily decreases from a value of 20 A/cm^2 at $B = 3$ T to less than 1 A/cm^2 at 13 T. This value of threshold is extremely low, even compared to record values $J_{\mathrm{th}} = 5$ A/cm^2 obtained from quantum box interband devices at similarly low temperatures [11]. This decrease in threshold current originates both from a reduction of the waveguide losses as well as from a strong increase of the gain, caused by the increase of the upper state lifetime with magnetic field. To understand more fully the behavior of the threshold current, we measured the threshold current density J_{th} in a series of five samples of various lengths between $L =$ 4.7 mm and $L = 1.8$ mm, extracting the waveguide loss α_w and gain $g\Gamma$ [12].

Waveguide losses and modal gain are plotted as a function of magnetic field in Fig. 2(a) for 420 μm wide laser stripes [13]. Two regimes are apparent. The main waveguide loss mechanism is, at these low THz frequencies, free carrier absorption. We believe that this is effectively quenched by the localization of carriers induced by magnetic field. This phenomenon should become significant as soon as $\omega_c\tau > 1$, i.e., the cyclotron energy is larger than the broadening of the levels of the injector; this condition is well fulfilled at $B = 6$ T. At large fields ($B > 9.3$ T), the waveguide loss is limited by the metal waveguide and no further reduction of the loss is possible. However, the dielectric constant of the semiconductor is anisotropic owing to the Landau quantization, and therefore an exact solution for the waveguide behavior is difficult . Solutions have been proposed for specific geometries different from ours [14]. However, in our geometry where the field is constrained by two metal boundaries it would be difficult to change significantly the field distribution. An experimental indication of this unchanged field distribution is that the group velocity refractive index $n_g = 3.9$, obtained from the spacing of longitudinal Fabry-Perot modes, does not change with magnetic field [see inset Fig. 2(b)]. It agrees well with the computed value ($n = 3.83$) using the $n = 2$ TM mode and tabulated refractive index values [15].

Below $B = 9.3$ T, the measured modal gain, displayed in Fig. 2(b), exhibits the same oscillations as the laser emission due to the modulation of lifetimes in the excited subbands caused by the coupling of the Landau levels. Specifically, we observe a decrease of the gain and lifetime by a factor of 2 at the field (9.3 T) where resonant *e-e* scattering is occurring. Above 9.3 T, gain increases dramatically by a factor of 5, attributed to an increase of the lifetime of the upper state by the same factor. Shown, alongside the gain data, is the lifetime deduced from magnetotransport measurements of the diagonal THz emitter studied in Ref. [16] with an energy spacing of 14 meV, very close to the energy spacing $E_{31} = 12.9$ meV of our laser. The behavior of the two quantities is very similar, confirming a dependence of the gain on the overall lifetime τ_3.

The origin of this strong increase in the lifetime may be understood by looking at the dependence of the threshold current density from magnetic field and temperature. In Fig. 3, the threshold current density is shown between 4.2 and 65 K for the various magnetic fields corresponding to a local maxima in the optical intensity.

For magnetic field below 6 T or temperatures above about 20 K, the threshold current density remains above a value of 10 A/cm^2, increasing as the temperature is raised and showing a very weak temperature dependence below 50 K. This is the behavior exhibited by all THz quantum cascade lasers [17], and reflects the increase in threshold current density caused by the activation of

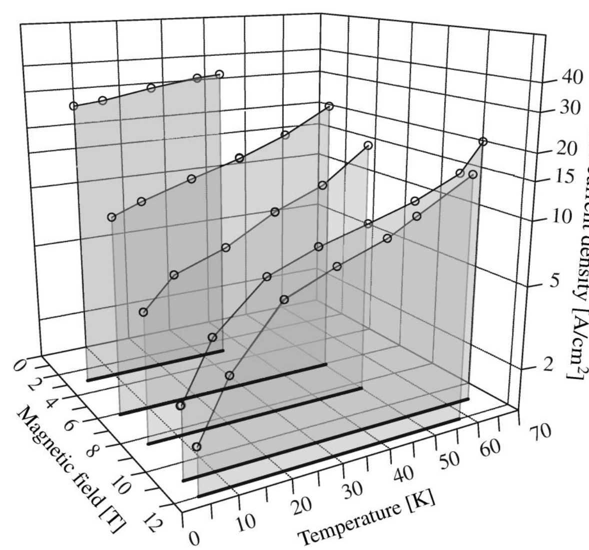

FIG. 3. Dependence of threshold current density on temperature and magnetic field for a 3.5 mm, 320 μm wide device. The change in lasing regime is evident above 6 T and below 20 K. The measurements at 4.2 K are performed with the sample immersed in liquid He.

optical phonon processes above a temperature of about 50 K. However, in our sample, for low temperatures and large magnetic fields, a strong reduction of threshold current density is observed, with the threshold varying by a factor of 5 between 4.2 and 20 K. This temperature range corresponds to an energy much lower than the cyclotron energy, but is compatible with the typical localization energy of $\approx$1 meV resulting from residual disorder in the sample.

From knowledge of the dipole matrix element, and measurement of the waveguide and mirror losses, an estimated upper state sheet density of $n_3 \simeq 1.24 \times 10^8$ cm^{-2} is obtained [18]. This corresponds to an effective upper state lifetime of $\tau_3 \approx 20$ ps and an average interelectron distance of 0.89 μm. Furthermore, recent work has shown that the localization of electrons on such a scale does occur even at much lower magnetic fields [19]. In reality, the situation is more complex than this since each of these electrons pockets will be coupled by tunneling to a common reservoir of electrons in the lower injector state, where a sheet density of $n_{\mathrm{inj}} = 5.3 \times 10^{10}$ cm^{-2} resides.

The nature of the main nonradiative channel between subbands, key to the performance of THz quantum cascade emitters at low temperatures, is still a matter of controversy. The observation in our data of clear electron-electron scattering resonances points to the importance of this process and is in agreement with indirect evidence obtained from light-current characteristics of nonlasing structures based on a vertical transition in a square well [20], whereas such behavior has never been observed in chirped superlattice or bound-to-continuum structures [21,22]. Actually, the largest increase in gain and lifetime is observed at large magnetic fields and low temperatures, i.e., in a situation where interface roughness and impurities do not lead to intersubband scattering but to an inhomogeneous broadening of the gain because of carrier localization. It is worth noting that this localization is at least as efficient for high excited states since the population inversion improves with magnetic field. Electron-electron scattering is also efficiently suppressed except for the resonant condition at 9.3 T [23].

In conclusion, our data show that extremely long intersubband lifetimes may be observed when well separated Landau levels are localized by a disorder potential—typical conditions for the quantum Hall effect. As the devices are very large compared to the wavelength, the very low threshold current densities would lead to a "thresholdless" device if structures could be fabricated in a microcavity configuration where the parameter β, the fraction of the spontaneous emission emitted in the lasing mode, is close to unity [24]. Our data also open up the very interesting possibility of observing effects such as Coulomb charging relating to the discreteness of the charge residing in localized islands.

The authors would like to acknowledge Marcel Graf for his help. This work was supported by the Swiss National Science foundation for Research, the EC project WANTED, EPSRC (UK), and Toshiba Research Europe Ltd.

*Electronic address: giacomo.scalari@unine.ch
†Present address: Alpes Lasers SA, 1-3 Maximilien-de-Meuron, CH-2000 Neuchâtel, Switzerland.
‡Electronic address: jerome.faist@unine.ch

[1] J. Faist *et al.*, Science **264**, 553 (1994).
[2] D. Smirnov *et al.*, Phys. Rev. B **66**, 121305 (2002).
[3] G. Scalari *et al.*, in Proceedings of the 26th International Conference on the Physics of Semiconductors, 2002 (unpublished).
[4] J. Alton *et al.*, Phys. Rev. B **68**, 081303 (2003).
[5] V. Tamosiunas *et al.*, Appl. Phys. Lett. **83**, 3873 (2003).
[6] G. Scalari *et al.*, Appl. Phys. Lett. **83**, 3453 (2003).
[7] G. Boebinger *et al.*, Phys. Rev. Lett. **65**, 235 (1990).
[8] M. Raikh and T. Shabazyan, Phys. Rev. B **49**, 5531 (1994).
[9] S. Blaser, M. Rochat, M. Beck, D. Hofstetter, and J. Faist, Appl. Phys. Lett. **81**, 67 (2002).
[10] K. Kempa *et al.*, Phys. Rev. Lett. **88**, 226803 (2002).
[11] Z. Alferov, Rev. Mod. Phys. **73**, 767 (2001).
[12] We used the expression of the threshold current densityJ_{th} in function of the waveguide losses α_w and the cavity length $L: J_{\mathrm{th}} = \frac{1}{g\Gamma}[\alpha_w - \frac{1}{L}\ln(R)]$, where $R = 0.67$ is the facet reflectivity calculated with a mode matching model. See, for example, C. Sirtori, J. Faist, F. Capasso, D. Sivco, A. Hutchinson, and A. Cho, IEEE J. Quantum Electron. **33**, 89 (1997).
[13] The calculation of the gain and losses over the whole set of five lasers is possible only above 5.5 T, because for the shortest cavity length there is no laser action at 2.9 T.
[14] V. Gvozdnikov and R. Vega-Monroy, Low Temp. Phys. **25**, 802 (1999).
[15] E. Palik, *Handbook of Optical Constants of Solids* (Academic Press, Orlando, Florida, 1985).
[16] S. Blaser, M. Rochat, M. Beck, J. Faist, and U. Oesterle, Phys. Rev. B **61**, 8369 (2000).
[17] R. Köhler *et al.*, Nature (London) **417**, 156 (2002).
[18] With the parameters $n = 3.9$, $2\gamma_{32} = 0.7$ meV, $\lambda = 159$ μm, $L = 0.35$ cm, $\alpha_w = 1$ cm^{-1}, $L_{\mathrm{per}} = 1701$ Å, $z_{ij} = 119.86$ Å, $\Gamma = 0.29$, $R_1 = 0.67$, $R_2 = 0.98$ (backfacet HR coated) we can calculate the upper state sheet density $\Delta n = (\epsilon_0 n\lambda 2\gamma_{32}L_{\mathrm{per}}/4\pi e^2 z_{ij}^2)(\frac{1}{\Gamma})(\alpha_w + \frac{1}{2L} \times \ln\frac{1}{R_1R_2}) = 1.24 \times 10^8$ cm^{-2}.
[19] S. Ilani *et al.* Nature (London) **427**, 328 (2004).
[20] M. Rochat, J. Faist, M. Beck, U. Oesterle, and M. Ilegems, Appl. Phys. Lett. **73**, 3724 (1998).
[21] G. Scalari *et al.*, Appl. Phys. Lett. **82**, 3165 (2003).
[22] R. Köhler *et al.*, Appl. Phys. Lett. **80**, 1867 (2002).
[23] A similar resonance arising between $n = 2$ and $n = 1$ states may be the origin of the abrupt increase in light intensity above 5.5 T when the condition $2E_{21} = \hbar\omega_c$ is satisfied, reducing the lower state lifetime. No features are to be expected in the conductance data in this case since the $n = 3$ lifetime is not affected.
[24] I. Protsenko *et al.*, Phys. Rev. A **59**, 1667 (1999).